PHYSICAL REVIEW B **69**, 132502 (2004)

Electronic structure of $CaCuO_2$ from the B3LYP hybrid density functional

Xiao-Bing Feng[1] and N. M. Harrison[2]
[1]*Department of Physics, Dalian Railway Institute, Dalian 116028, People's Republic of China*
[2]*Department of Chemistry, Imperial College of Science, Technology and Medicine, London SW7 2AY, United Kingdom*

(Received 8 August 2003; revised manuscript received 18 December 2003; published 12 April 2004)

The electronic structure of the infinite layer compound $CaCuO_2$ has been calculated with the B3LYP hybrid density functional. The mixing of the Hartree-Fock (HF) exchange into the exchange-correlation energy separated the bands crossing Fermi energy to form an antiferromagnetic insulating ground state of charge transfer type. The elimination of the self-interaction through the HF exchange and the optimized correlation energy have significantly improved theoretical results. The theoretical energy gap and magnetic moment are in excellent agreement with the experiments. The ratio of intralayer to interlayer magnetic coupling constants and lattice parameters are also in good accordance with the experiments. Some characteristics of the electronic structure of insulating $Sr_2CuO_2Cl_2$ from angle-resolved photoemission experiments are observed in the band structure of $CaCuO_2$.

DOI: 10.1103/PhysRevB.69.132502 PACS number(s): 74.25.Jb, 71.15.Mb, 71.27.+a

I. INTRODUCTION AND METHOD

As a parent compound of high-temperature superconductors (HTSC's), the infinite layer material $CaCuO_2$ (Ref. 1) has a simple structure and a high-transition temperature when doped to optimum hole density.[2] Similar to La_2CuO_4 and $YBa_2Cu_3O_6$, $CaCuO_2$ has an insulating three-dimensional antiferromagnetic (AFM) ground state,[3] with energy gap $\Delta = 1.5$ eV (Ref. 4) and magnetic moment $\mu = 0.51\mu_B$.[3] Although the ratio of interlayer to intralayer magnetic coupling is one order of magnitude higher than that in La_2CuO_4 and $YBa_2Cu_3O_6$, the ratio is still very low. The nuclear magnetic resonance experiment on Cu in $Ca_{0.85}Sr_{0.15}CuO_4$ shows that the interlayer coupling is about two orders of magnitude less than the intralayer one.[5]

The electronic structure of $CaCuO_2$ has been investigated by several theoretical methods, such as linearized augmented plane wave method,[6] linear muffin tin orbital atomic sphere approximation,[7] full potential linear muffin tin orbital method.[8] These methods are based on the local spin-density approximation (LSDA); they failed to give the correct ground state, as in the case of other parent HTSC's.[9] Later, it was found that the failure was due to the self-interaction inherent in the LSDA density functional, which tends to delocalize the electrons. The self-interaction correction (SIC) method gave correct AFM insulating ground state with $\mu = 0.58\mu_B$ and $\Delta = 0.84$ eV.[10] The LSDA+U method also generated correct ground state, with $\Delta = 2.1$ eV and $\mu = 0.66\mu_B$ for $U = 7.5$ eV (Ref. 11) and $\Delta = 1.96$ eV and $\mu = 0.71\mu_B$ for $U = 5$ eV.[12] Although the two approaches recovered the correct ground state, their quantitative comparisons with the experiments were not satisfactory.

In this paper we study the electronic structure of $CaCuO_2$ with the so-called B3LYP hybrid density functional.[13] The B3LYP hybrid functional was very successful in the thermochemistry of atoms and molecules. Recently, the hybrid functional was applied to some periodic systems.[14,15] The argument for mixing the Hartree-Fock (HF) exchange in the exchange-correlation energy E_{XC} is based on the adiabatic connection formula.[13] In the so-called B3LYP scheme the Perdew-Wang[16] gradient-corrected correlation energy is replaced by Lee-Yang-Parr correlation energy.[17] The B3LYP exchange-correlation energy functional reads

$$E_{XC} = E_X^{LSDA}(1-a_0) + a_0 E_X^{exact} + a_X \Delta E_X^{B88} + E_C^{LSDA} + a_C \Delta E_C^{LYP}, \quad (1)$$

in which the local spin-density functional of Vosko, Wilk, and Nusair[18] is used for E_X^{LSDA} and E_C^{LSDA}. E_X^{exact} is the exact nonlocal HF exchange energy. ΔE_X^{B88} and ΔE_C^{LYP} are the Becke's[19] and Lee-Yang-Parr's gradient corrections for the local exchange and correlation energies, respectively. The weight coefficients for the gradient-corrected correlation energy, local exchange energy, and the exact HF exchange terms were determined by a linear least-square fitting of the thermochemical properties of some atoms and molecules to the experiments. The atom with highest atomic number used in the fitting is Cl. No atoms with d or higher shells were used. Twenty percent of the exact HF exchange energy in the exchange-correlation energy gives theoretical results in good agreement with experiments. The optimum values for the parameters a_0, a_X, and a_C are 0.20, 0.72, and 0.81, respectively.[13] We keep the original weight coefficients and treat the functional as a parameter-free one.

In this paper the calculations are carried out with CRYSTAL package.[20] The basis vectors for expanding the Kohn-Sham orbitals are Bloch functions composed of localized contracted basis sets.[21] All-electron basis sets for Ca, Cu, and O ions are of the form of 86-511G, 86-411(41d)G, and 8-411G, respectively. In the calculations 75 points in the irreducible part of the first Brillouin zone (FBZ) were used. We adopt the 7, 7, 7, 7, and 14 as the integral tolerances to obtain high precision in monoelectronic and bielectronic integrals. Also strict criteria for convergence, i.e., when the difference between two consecutive root-mean-squared values of the density-matrix elements is less than 10^{-9} the convergence is assumed, are used to make the magnetic moments on Cu sites converge. Different magnetic states, i.e., metallic (without spin polarization), ferromagnetic, two-

TABLE I. The energy gaps Δ (in eV) and magnetic moments μ (in μ_B) from different theoretical schemes are compared with experiments for $CaCuO_2$ and La_2CuO_4.

	UHF	SIC-LSD	LSDA+U	B3LYP	Expt.
$CaCuO_2$ (Δ)	14.9	0.84 (Ref. 10)	2.1 (Ref. 11) 1.96 (Ref. 12)	1.54 [a] 1.50 [b]	1.5 (Ref. 4)
$CaCuO_2$ (μ)	0.89	0.58 (Ref. 10)	0.66 (Ref. 11) 0.71 (Ref. 12)	0.51 [a] 0.51 [b]	0.51 (Ref. 3)
La_2CuO_4 (Δ)	17 (Ref. 24)	2.1 (Ref. 25) 1.04 (Ref. 23)	1.65 (Ref. 26)	2.0 (Ref. 15)	2.0 (Ref. 27)

[a] Obtained using experimental lattice parameters.

[b] Obtained using optimized lattice parameters.

dimensional (2D), and three-dimensional (3D) antiferromagnetic structures, were checked to find the ground-state magnetic configuration. For comparisons, the unrestricted Hartree-Fock (UHF) and general gradient-corrected LSDA (LSDA+GGA) calculations were also carried out with the same basis sets. We also performed structural optimization for the 3D AFM supercell. The optimization is implemented with Domin algorithm and the P4/mmm symmetry is preserved.

II. RESULTS AND DISCUSSION

Our results show that the 3D AFM state has the lowest energy, i.e., the B3LYP hybrid functional could predict correct ground-state magnetic configuration. The energy difference per unit cell between the ferromagnetic and the 2D AFM (antiferromagnetic order in the CuO_2 plane and ferromagnetic order in the Z direction) ground state is 0.285 eV. The 2D and 3D AFM states have nearly the same energies, with the energy of 3D AFM state only 0.001 64 eV lower than that of 2D AFM state. The energies of different magnetic configurations could be described by the Ising model,

$$E=\sum_{\langle ij\rangle} J_{ij}S_iS_j\,. \tag{2}$$

The intralayer coupling constant $J_\parallel$ and interlayer coupling constant $J_\perp$ could be obtained from the energy differences of the three different magnetic states. One can easily get $J_\parallel=[E_{FM}-E_{2DAFM}]/4$ and $J_\perp=[E_{2DAFM}-E_{3DAFM}]/2$, in which E_{FM}, E_{2DAFM}, and E_{3DAFM} are the energies of FM, 2D AFM, and 3D AFM states, respectively. The theoretical results are $J_\parallel=825.5$ K and $J_\perp=9.49$ K. The ratio $J_\perp/J_\parallel$ is 1.1%, which is in good agreement with the experimental result that the interlayer magnetic coupling is about two orders of magnitude weaker than the intralayer coupling.[5]

The optimized lattice parameters for the supercell are $a=5.563$ Å and $c=6.536$ Å. The results are about 2% larger than the experimental values.[1] The precision is comparable to LDA computations for conventional materials. In addition, Table I shows that the B3LYP theoretical magnetic moments and energy gap obtained with experimental and theoretical lattice parameters are in excellent agreement with the experiments.[3,4] As mentioned above the optimum parameters were obtained with atoms and molecules without d electrons, so the excellent agreement between the theory and experiments was unexpected because of the strong localized character of d orbitals. But from the study of pseudopotentials one knows that the $2p$ orbitals in the first-row atoms also pose problems, these orbitals have also localized character because of the lack of orthogonal repulsions. So, if there are enough variational freedoms in the B3LYP hybrid functional to correctly describe atoms with $2p$ shell then it could be applied to systems with $3d$ electrons.

The large energy gap of the UHF results from the lack of correlation, i.e., the interaction is not screened. As can be seen in Table I, the UHF gaps for both $CaCuO_2$ and La_2CuO_4 are about one order of magnitude larger than the experimental results. It is also much larger than the usual cases, which means that the correlation effects are more important in these materials. Conventional local-density approximation to the density functional theory (DFT) underestimates over 30% the energy gaps of semiconductors. The fact is usually ascribed to the inability of DFT to calculate the properties of excited states of materials, for DFT is initially invented to study properties of the ground state. The B3LYP results for energy gaps of semiconductor of various bonding types, such as Si, GaAs, ZnO, TiO_2, etc., are in excellent agreement with experiment.[14] In addition to $CaCuO_2$ and La_2CuO_4, the B3LYP energy gaps for some other strongly correlated electronic systems, such as MnO and NiO, are also in good agreement with experiment.[14] The good agreement of B3LYP results with experiment may not be accidental. A theorem similar to the Koopmann's theorem in UHF is yet to be established.

The projected densities of states (DOS's) are shown in Fig. 1 and the band structures along the high symmetry lines are shown in Fig. 2(a). These results are obtained with experimental structural parameters. The results show that $CaCuO_2$ is a charge transfer insulator. This is similar to the case of transition metal monoxides.[14] As shown in Fig. 1 the main components at the top of the valence bands and the bottom of the conduction bands are Cu $3d_{x^2-y^2}$ and O $2p_{x(y)}$. Though the spectral weight at the bottom of the conduction bands is mostly of Cu $3d_{x^2-y^2}$ nature, there is a significant ingredient of O $2p_{x(y)}$ at the top of the valence bands. Because of the lack of apical oxygens in $CaCuO_2$ the bonding along the Z direction is weak, which is different from La_2CuO_4, where significant Cu $3d_{z^2}$/O $2p_z$ compo-

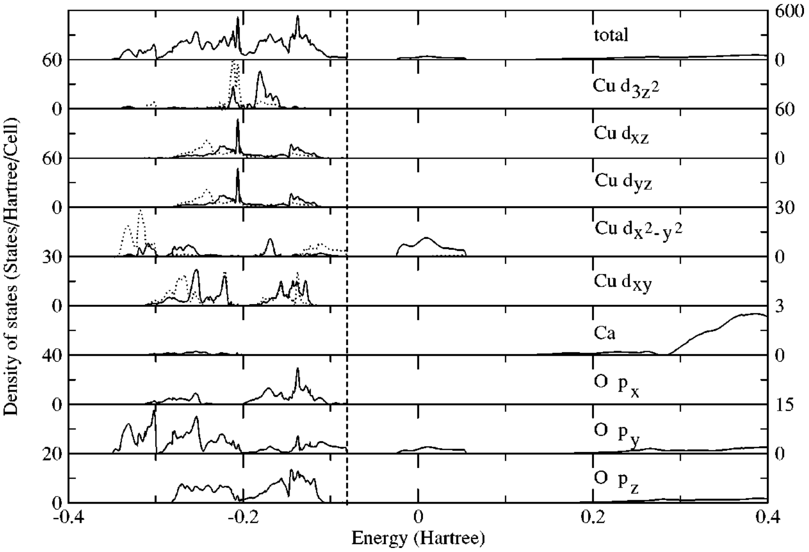

FIG. 1. The projected densities of states of Cu $3d$, O $2p$, and Ca $3sp$ partial waves in a $\sqrt{2}\times\sqrt{2}\times 2$ supercell of $CaCuO_2$. The magnetic moment of Cu is $-0.51\mu_B$. The dotted lines represent the DOS's for spin-down electrons.

nents are existent at the top of the valence bands.[15] The result suggests that the Cu $3d_{z^2}$/O $2p_z$ components in La_2CuO_4 may not be essential to the high-temperature superconductivity of the system.

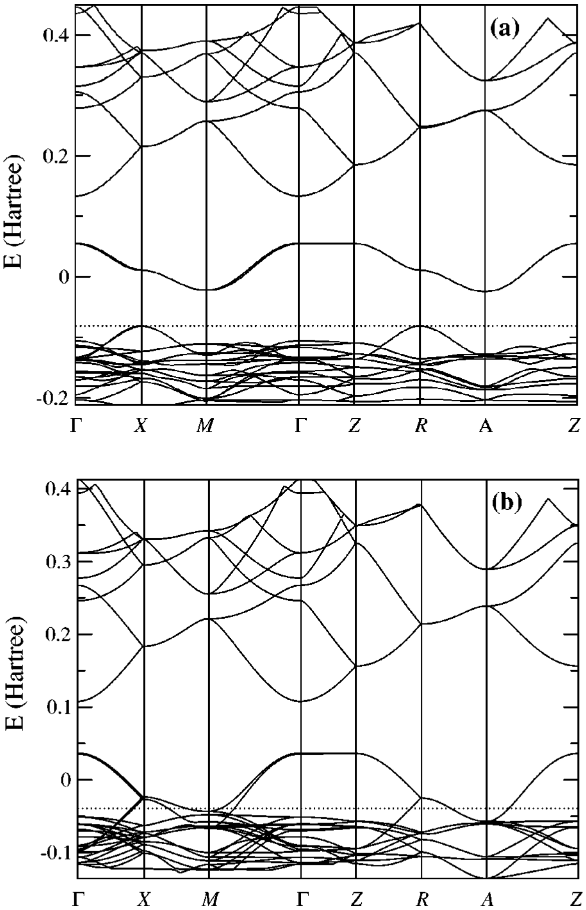

FIG. 2. The B3LYP energy bands of a $\sqrt{2}\times\sqrt{2}\times 2$ supercell of $CaCuO_2$. (b) The GGA band structure of the same supercell. The Fermi energy and the top of valence bands are denoted by dotted lines.

One may also notice that some features in Fig. 2(a) are in good agreement with the angle-resolved photoemission (ARPES) experiments on the insulating $Sr_2CuO_2Cl_2$.[28] $Sr_2CuO_2Cl_2$ has a structure similar to La_2CuO_4, with the apical oxygens in La_2CuO_4 replaced by Cl.[29] The X and M points in Fig. 2(a) correspond to the ($\pi/2$, $\pi/2$) and (π, 0) points in the FBZ of the CuO_2 plane, respectively. The (π, π) point in the ARPES experiments is equivalent to Γ point in Fig. 2(a). The ARPES experiments show that the valence-band top is at ($\pi/2$, $\pi/2$) and there is a nearly isotropic dispersion around this point. The dispersion from (π, 0) to (0, 0) is flat and the dispersion from (π, 0) to (0, π) is similar to the one from (0, 0) to (π, π). All these characteristics are consistent with our results, as can be seen in Fig. 2(a). Due to the folding-up of the FBZ in the case of the AFM supercell, there are two nearly degenerate bands around X points. Although the dispersion along the Γ-X-M direction in Fig. 2(a) is stronger than experimentally observed, a better agreement with experiments may be expected by applying the method to $Sr_2CuO_2Cl_2$.

To see the effect of the mixing of the exact exchange the LSDA+GGA band structure is shown in Fig. 2(b) for comparison. The same supercell and same functionals for GGA corrections were used in the LSDA+GGA and the B3LYP calculations. From Fig. 2(a) and Fig. 2(b) one can see that the mixing of the exact exchange results in no significant change of the dispersions and relative positions of the bands far from Fermi energy E_F. But the important effect of mixing exact exchange is that two bands, which cross E_F, are separated from the other two bands. The separated two bands have no overlap with the other conduction bands, which is different from the LSDA+U results.[11,12] In the LSDA+U scheme there are also two separated bands composed of Cu $3d_{x^2-y^2}$ and O $2p_{x(y)}$ antibonding states, but the two bands are overlapped with other conduction bands.[12]

Except the difference mentioned above between the B3LYP and the LSDA+U schemes, some essential characters are shared by the two approaches. The reduced energy gap results from upward shift of part of Cu $3d_{x^2-y^2}$ and O

$2p_{x(y)}$ spectral weights, and this part of spectral weights have similar width in both schemes. Also the most important projected DOS's for Cu $3d_{x^2-y^2}$ and O $2p_{x(y)}$ have the same characters.[11] Although the LSDA+U captures the essential physics in strongly correlated systems its quantitative results are not as good as the B3LYP. The reason may be due to the simple mean-field treatment of the Hubbard U term in the LSDA+U.

In the LSDA+U scheme it is easy to see the reason why the bands crossing E_F were separated to form a gap. The additional orbital dependent potential splits a band into Hubbard subbands, with separation equal to approximately the screened on-site Coulomb repulsion U. The SIC approach restores the localized character of d orbitals, thus introducing strong on-site Coulomb repulsion. In the studies of the Mott insulators it was found that the simple UHF can give qualitatively correct results, whereas more advanced DFT methods failed.[22] The reason is that in the UHF there is no self-interaction.

In our UHF calculation for $CaCuO_2$ the energy gap is about one order of magnitude larger than the experimental result. It is expected that a small amount of mixing of the exact exchange would reduce the unphysical large gap to the experimental value while maintaining the correct ground-state magnetic configuration. But in the B3LYP approach it is not very clear why only 20% mixing of the exact exchange into the GGA corrected LSDA can greatly change the LSDA +GGA results. To see the point one can rewrite Eq. (1) as

$$E_{XC}=E_X^{exact}+(1-a_0)(E_X^{LSDA}-E_X^{exact})+a_X\Delta E_X^{B88}+E_C^{LSDA}+a_C\Delta E_C^{LYP}. \tag{3}$$

Instead of only 20% exact exchange one can view the B3LYP as incorporating 100% exact exchange, and treat the second and the third terms as additional contributions to the correlation energy. So, with the exact exchange, where the self-interaction is excluded, and additional variation freedoms for correlation energy one should expect that the method would give better results than GGA and UHF do, in the latter case the correlation energy is totally discarded.

One may view the B3LYP hybrid functional as a much improved energy functional towards the exact one. Some important issues in high-temperature superconductors, such as stripe phase, may also be studied with the hybrid density-functional method in which charge and spin density are basic quantities independent of the Kohn-Sham quasiparticle picture.

III. CONCLUSION

To conclude, the B3LYP hybrid density functional has been applied to $CaCuO_2$. The mixing of the exact exchange reduced the self-interaction and caused the band separation about the Fermi energy. The magnetic moment and energy gap are in excellent agreement with experiment. Lattice parameter and magnetic coupling constants are also in good agreement with experiment. The ARPES characteristics on $Sr_2CuO_2Cl_2$ are observed in our calculations on $CaCuO_2$.

---

[1] T. Siegrist *et al.*, Nature (London) **334**, 231 (1988).
[2] M. Azuma *et al.*, Nature (London) **356**, 775 (1992).
[3] D. Vaknin *et al.*, Phys. Rev. B **39**, 9122 (1989).
[4] Y. Tokura *et al.*, Phys. Rev. B **41**, 11 657 (1990).
[5] A. Lombardi *et al.*, Phys. Rev. B **54**, 93 (1996).
[6] L.F. Mattheiss and D.R. Hamann, Phys. Rev. B **40**, 2217 (1989); D. Singh *et al.*, Physica B **163**, 470 (1990).
[7] M.A. Korotin and V.I. Anisimov, Mater. Lett. **10**, 28 (1990).
[8] D.L. Novikov *et al.*, Physica C **210**, 301 (1993).
[9] W.E. Pickett, Rev. Mod. Phys. **61**, 433 (1989).
[10] D. Singh *et al.*, Physica C **162-164**, 1431 (1989).
[11] V.I. Anisimov *et al.*, Phys. Rev. B **44**, 943 (1991).
[12] H. Wu *et al.*, J. Phys.: Condens. Matter **11**, 4637 (1999).
[13] A.D. Becke, J. Chem. Phys. **98**, 5648 (1993).
[14] J. Muscat *et al.*, Chem. Phys. Lett. **342**, 397 (2001).
[15] J.K. Perry *et al.*, Phys. Rev. B **63**, 144510 (2001).
[16] J.P. Perdew, in *Electronic Structure of Solids*, edited by P. Ziesche and H. Eschrig (Academic Press, Berlin, 1991).
[17] C. Lee *et al.*, Phys. Rev. B **37**, 785 (1988).
[18] S.H. Vosko *et al.*, Can. J. Phys. **58**, 1200 (1980).
[19] A.D. Becke, Phys. Rev. A **38**, 3098 (1988).
[20] V.R. Saunders *et al.*, *CRYSTAL98 User's Manual* (University of Torino, Torino, 1998).
[21] See http://www.theochem.unito.it/teorica/crystal/Basis_Sets/mendel.html
[22] N.M. Harrison *et al.*, Philos. Trans. R. Soc. London, Ser. A: Math. Phys. Eng. Sci. **356**, 87 (1998).
[23] A. Svane, Phys. Rev. Lett. **68**, 1900 (1992).
[24] Y.-S. Su *et al.*, Phys. Rev. B **59**, 10 521 (1999).
[25] W.M. Temmerman *et al.*, Phys. Rev. B **47**, 11 533 (1993).
[26] M.T. Czyzyk and G.A. Sawatzky, Phys. Rev. B **49**, 14 211 (1994).
[27] J.M. Ginder *et al.*, Phys. Rev. B **37**, 7506 (1988).
[28] B.O. Wells *et al.*, Phys. Rev. Lett. **74**, 964 (1995); C. Kim *et al.*, *ibid.* **80**, 4245 (1998).
[29] L.L. Miller *et al.*, Phys. Rev. B **41**, 1921 (1990).